Absorption matrix for fusion in coupled reaction channel calculations

S. V. S. Sastry
Nuclear Physics Division, Bhabha Atomic Research Centre, Mumbai 400 085, India
(Received 10 February 2000; published 8 August 2000)

The absorption of flux for fusion from a coupled channels system has been examined over a wide range of energies. The full absorption matrix for fusion, consisting of the diagonal absorption and the fusion in transition, is presented. The fusion in transition is at times more than the removal of flux while propagating in the physical channels. The absorption matrix is obtained also for the case of purely real coupling potentials. The absorption matrix method is shown to be superior to the usual method of difference of cross sections used in some of the present coupled channels fusion codes. The flux absorbed within a given channel has been resolved into the constituent subchannels of the total angular momentum. Using this approach, the isocentrifugal approximation has been examined for various cases.

PACS number(s): 24.10.Eq, 25.70.Bc, 25.70.Hi, 25.70.Jj

The coupled reaction channels (CRC) formalism provides a simultaneous description of the elastic and all the reaction channels of the heavy ions scattering. In this formalism, the heavy ion fusion is estimated using two different approaches. The first approach is based on the transmission of flux through the (eigen) channel barriers as in [1], with the use of the isocentrifugal (ICA) approximation. The use of an analytical expression like the Hill-Wheeler transmission through a parabolic barrier shape as in [1] circumvents the need for numerical integration of the coupled equations to find the transmission. In the recent coupled channels (CC) fusion code CCFULL [2] which has several merits over that of [1], the transmission is found by integrating the equations through the barrier region, while retaining the ICA. Each (inelastic) channel coupled gives rise to several subchannels owing to the addition of spin (I) of the nucleus excited with the incoming orbital angular momentum (L). In the ICA, the kinetic energy operators of all inelastic channels are taken to be the same [3–7] by ignoring the spins of excited states. The centrifugal energy $L(L+1)\hbar^2/2\mu R^2$ of each channel is replaced in terms of channel total spin J by $J(J+1)\hbar^2/2\mu R^2$, whereas the coupling potentials depend on the multipolarity (λ) of the excitation. This scheme grossly reduces the number of coupled equations to a bare minimum, i.e., the number of channels considered in the coupling scheme. Consequently, the ICA rendered realistic CC fusion calculations feasible for complex systems, even before the advent of the high speed computers and for more elucidation, refer to an excellent discussion in [7] and the references therein.

In the second approach, fusion is estimated using a short ranged imaginary potential in each of the coupled channels to absorb flux for fusion, as used in the CC code ECIS [8] and the CRC code FRESCO [9]. The CRC iterations with real potentials and fusion imaginary potentials give a self-consistent solution consisting of the wave functions of various channels. Following the phase shift analysis, the S-matrix elements for all the channels are estimated. The difference between the total reaction (from elastic channel) and the cumulative cross sections of the remaining channels explicitly taken in the coupling scheme gives the fusion cross section, as given by Eq. (1) (for example, see [4]). This will be henceforth referred to as the phase shift (PS) method. The PS method is extremely sensitive to the CRC input parameters like the maximum radius, the radial step size and the accuracy for S-matrix elements, etc. ($R_{\max},\delta R,\delta S$), at energies below the Coulomb barrier [10]. Therefore, care should be exercised when following the PS method for fusion at submillibarn cross sections. The fusion calculations using the PS method for a limited coupling scheme showed good agreement with the results of the transmission method up to microbarn cross sections in [4,6]. Owing to the long ranged Coulomb couplings this agreement is not easily achieved in numerical calculations.

In the present work the merits of the PS and the absorption matrix (AM) methods for fusion are discussed. The main advantage of the PS method for fusion is that it needs no additional computations, as the fusion spin distribution is obtained from the available partial wave cross sections of various channels coupled. In order to understand the contribution of a particular channel, one therefore needs fusion without that channel and also the fusion including that channel, as tabulated in [11]. The difference between these two cross sections gives an estimate of fusion from that channel. However, it is not equivalent to the flux absorbed from a given channel when all other channels are also present in the coupling scheme. The AM method of Eq. (2), as given in Eq. (A2) of [11] and in Sec. 4.2 of [12], provides a method to understand the full absorption matrix for fusion together with the nondiagonal terms represented by $\sigma_{\rm tr}$ of Eq. (3). These transition terms for fusion arise due to the complex coupling potentials and vanish if the couplings are real. Using the AM method, it is possible to obtain the fusion spin distributions for any required channel in the presence of the full coupling scheme:

$$\sigma_f=\frac{\pi}{k^2}\sum_J (2J+1)\left[1-\sum_{\alpha\alpha'}\frac{k'\mu}{k\mu'}|S^J_{\alpha\alpha'}|^2\right], \qquad (1)$$

$$\sigma_a=\sum_{J,\alpha\beta}\sigma_a^{J,\alpha\beta}=\sum_{J,\alpha\beta}\frac{-2\pi}{\hbar v}(2J+1)\langle\chi_\alpha|W_{\alpha\beta}|\chi_\beta\rangle, \qquad (2)$$

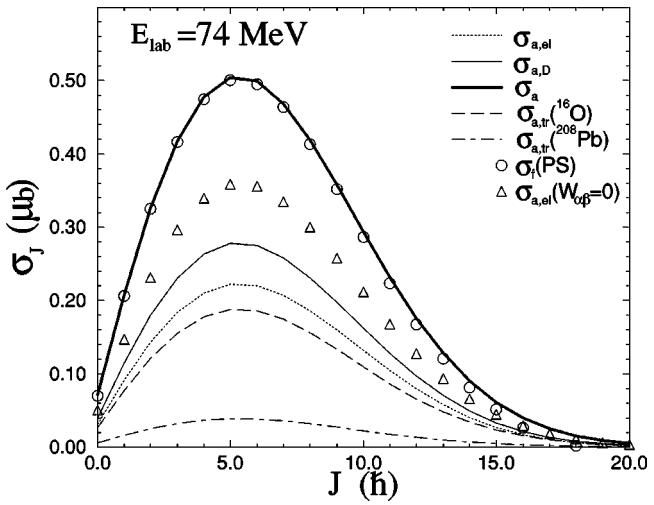

FIG. 1. Spin distributions of various components of the absorption matrix and a comparison of the AM and the PS methods.

$$\sigma_a = \sigma_{a,\mathrm{el}} + \sigma_{a,\mathrm{ne}} + \sigma_{a,\mathrm{tr}} \equiv \sigma_{a,D} + \sigma_{a,\mathrm{tr}}. \tag{3}$$

In the above, χ_α is the relative motion wave function of the channel α, v is the relative velocity in the entrance channel $\alpha=1$. It is known that the absorption of flux determined from the integrals of Eq. (2) is equivalent to the fusion estimated by Eq. (1), i.e., $\sigma_f=\sigma_a$. However, in practice it is not easy to establish this equality in the numerical calculations at low energies owing to different numerical accuracies of Eqs. (1) and (2). In the AM method, the flux absorbed from the coupled channels system truly represents fusion provided the fusion imaginary potentials are short ranged. For converged fusion estimates, the coupling scheme should include all other important reaction channels. In contrast to the PS method, Eq. (2) gives accurate results for fusion and is insensitive to $R_{\max}, \delta R, \delta S$ parameters. The inputs required for this method are already available in the CRC codes. It provides an additional advantage of understanding the fusion from each physical channel, especially for each angular momentum subchannel of a given block of total spin J [denoted by α' in Eq. (1)]. Therefore, the AM method can be used to understand the ICA made in various simplified codes for fusion such as Refs. [1,2]. Furthermore, Eq. (2) can also be used to understand the radial distributions of flux for fusion.

In the present model calculations we consider two different coupling schemes each consisting of three channels, using the code FRESCO [9]. In the first coupling scheme the elastic channel, the 3^- excited state of ^{16}O and the 3^- excited state of ^{208}Pb are considered and the results will be presented in Fig. 1. In the second scheme, the 3^- state of ^{208}Pb is replaced with the 5^- state of ^{208}Pb as will be shown in Figs. 2(a) and 2(b). The channels of these schemes are indexed by $\alpha=1,2\{\ldots\},3\{\ldots\}$, whereas $\{\alpha'\}$ represents the group of subchannels within α partition generated by the angular momentum couplings due to the spin I of the excited state, i.e., $J=L=I\otimes L'$ for the present work. The elastic channel is represented by $\alpha=1$ and for the present coupling schemes all $\{\alpha'\}$ belong to the same mass partition implying $\mu=\mu'$ in Eq. (1). The imaginary parts of the diagonal optical potentials, $(U_{\alpha\alpha}, W_{\alpha\alpha})$, result in the absorption of the waves propagating in the channels α. These are the short ranged fusion imaginary potentials of Woods-Saxon square form with $W_0=10.0$ MeV, $r_i=1.0$ fm and $a_i=0.4$ fm [11]. The coupling potentials $(U_{\alpha\beta}, W_{\alpha\beta})$ for $\alpha\neq\beta$ are derived by deforming the diagonal parts of the optical potentials. The absorption of flux for fusion from the coupled channel system is generated by these $W_{\alpha\beta}$. The need for the complex coupling potentials is discussed in [13]. In the following, we present our study for various cases of (1) absorption from the elastic channel given by $\alpha=\alpha'=1$ of Eq. (2), and represented by $\sigma_{a,\mathrm{el}}$ of Eq. (3); (2) cumulative absorption from all the diagonal terms of the absorption matrix given by $\{\alpha,\beta\}=\{\alpha,\alpha\}$ and $\{\alpha',\alpha'\}$ as represented by $\sigma_{a,D}$ of Eq. (3); (3) full absorption with the inclusion of the nondiagonal terms for the absorption given by all the values of α and β as represented by σ_a, the full right side of Eq. (3); (4) fusion predicted by the PS method using Eq. (1); and (5) absorption taking place in the α' subchannels of a J block.

Figure 1 illustrates the merits of the AM method compared to the PS method at a low energy. The dotted curve represents the absorption from the coupled elastic channel, which is found to be much higher than the absorption from any other channel. The dashed line and dash-dotted lines represent fusion in transition [σ_{tr} of Eq. (3)], taking place from the excited states of ^{16}O and ^{208}Pb, respectively. This includes the contribution from all the partial waves leading to a total angular momentum J. The solid curve represents the total diagonal absorption of case (2) listed above. The thick solid curve represents the full absorption for fusion

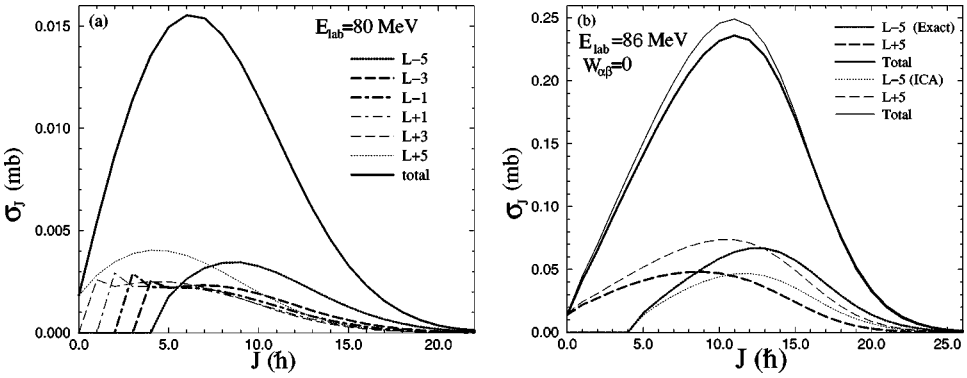

FIG. 2. (a),(b) Partial wave distributions of various subchannels leading to a given J, of Pb excited state at two energies, as discussed in text.

TABLE I. Comparision of fusion predictions of the AM and the PS methods as a function of L_c.

$E_{\rm lab}$ MeV	L_c ($\hbar$)	$\sigma_{a,\rm el}$ mb	$\sigma_{a,D}$ mb	$\sigma^o_{a,\rm tr}$ mb	σ_a mb	$\langle L^2\rangle$ $\hbar^2$	σ_f mb	$\langle L^2\rangle$ $\hbar^2$
76.0	10	0.03	0.04	0.026	0.07	43.8	0.071	43.8
	15	0.04	0.05	0.031	0.08	63.2	0.084	63.2
	20	0.04	0.05	0.032	0.09	69.0	0.086	68.7
	30	0.04	0.05	0.032	0.09	69.6	0.086	68.2
	40	0.04	0.05	0.032	0.09	69.6	0.086	66.9
78.0	10	0.45	0.57	0.37	1.02	44.6	1.01	44.8
	20	0.55	0.70	0.46	1.26	72.4	1.21	66.4
	30	0.56	0.71	0.46	1.26	73.3	1.21	67.3
	40	0.56	0.71	0.46	1.26	73.3	1.22	67.2
	50	0.56	0.71	0.46	1.26	73.3	1.22	67.3
80.0	10	4.32	5.52	3.45	9.74	47.1	9.78	47.1
	20	5.61	7.18	4.53	12.71	81.7	12.71	81.4
	30	5.63	7.20	4.54	12.75	83.2	12.86	87.7
	40	5.63	7.20	4.54	12.75	83.2	12.98	99.0
	60	5.63	7.20	4.54	12.75	83.2	13.11	120
83.0	10	24.6	31.5	19.2	54.7	57.6	55.4	57.7
	20	48.2	61.7	38.3	108.0	137.3	109.4	137
	30	49.0	62.8	39.1	110.0	144	111.4	144
	40	49.0	62.8	39.1	110.0	144	111.5	146
86.0	10	27.3	37.1	21.4	62.7	59.9	62.9	59.8
	20	91.8	120.9	73.1	208.4	207	209.8	207
	30	108.9	143.0	87.7	248.2	261	250.1	261
90.0	10	22.9	36.3	16.4	59.5	60.2	59.7	60.1
	20	87.2	130.9	65.3	217.4	220	217.8	220
	30	168.8	239.3	133.7	408.5	423	410.7	424
	40	172.4	244.2	137.2	417.7	437	420.0	438
96.0	10	21.0	42.2	10.9	58.4	59.6	58.3	59.7
	20	61.9	132.5	52.4	205.2	217	205.1	217
	30	156.4	274.9	122.8	441.5	475	441.3	475
	40	235.3	384.6	195.3	639.6	701	639.4	702

representing case (3). The circles represent the spin distribution from the PS method of case (4), showing a good agreement of these two methods at various energies in the present work. The wave functions for the AM method were generated using $R_{\rm max}=17.0$ fm, $\delta R=0.1$ fm, and $\delta S=0.01$ (set 1). The results were found to be stable for all the 100 partial waves considered. The results of the PS method for the same parameters (set 1) are not in agreement with the thick solid curve of Fig. 1 at energies below the Coulomb barrier, whereas this agreement improves for energies above 78 MeV. The circles of Fig. 1 represent the converged results of the PS method and were generated using $R_{\rm max}=30.0$ fm, $\delta R=0.025$ fm, and $\delta S=0.0000001$ (set 2), needing more computation time and memory. Further, the calculations using the set 2 did not converge for fusion for the partial waves beyond $20\hbar$ and are not shown in the Fig. 1 as they are negative. The results of the PS method for fusion have been shown in Table I, represented by σ_f and $\langle L^2\rangle$ in the last two columns. The parameter set 2 has been used for the energy range 66–78 MeV (listed from 76 MeV in the table) and the set 1 for energies above 78 MeV. The use of set 1 for energies below 76 MeV results in large fusion cross sections of millibarns by the PS method, for example, at 74 MeV it is mostly beyond the upper bound of Fig. 1. The PS method needs a cutoff L value (L_c) for fusion at low energies, as its predictions change drastically with increasing L_c. In contrast, the AM method in Eq. (2) yielded converged results around $L_c\approx 30\hbar$ and did not change by increasing L_c to $100\hbar$. The mean square spin for the absorption from the elastic channel, the total diagonal absorption and the full absorption cases are roughly the same at low energies as listed in column 7 of the table, which differ at above barrier energies. For example at 96 MeV incident energy, the converged values with $L_c=50\hbar$, are 741.1, 672.9, and 703.2 $\hbar^2$, respectively. The absorption of flux into the fusion channel through all the transition terms for $\alpha\neq\beta$ of Eq. (2) for a given J is not negligible. This can be understood from the difference of full and diagonal absorptions, i.e., of columns 6 and 4 of the table. The contribution to the transition terms from the oxygen inelastic partition is listed in the table in column 5.

When the imaginary parts of the coupling potentials are switched off (i.e., $W_{\alpha\beta}=0$ for $\alpha\neq\beta$) the nondiagonal terms of Eq. (2) vanish. This results in a redistribution of flux for fusion in various diagonal terms as also discussed in (Table II of) [11]. In this case, the absorption from elastic channel increases as shown by the triangles in Fig. 1. The total diagonal absorption of this case agrees with the full absorption curve of Fig. 1. Furthermore, it has been observed that deformation of the short ranged imaginary potentials does not effect the results of the fusion or the other channels. For this case of $W_{\alpha\beta}=0$ for $\alpha\neq\beta$, the AM method becomes simple and only the diagonal terms need to be evaluated.

Figures 2(a) and 2(b) show the absorption as a function of total angular momentum J at below barrier and above barrier energies. The various curves show the absorption from the individual partial wave subsets of J, for the 5^- excited state of ^{208}Pb using the second coupling scheme. All these calculations have been performed for both the coupling schemes mentioned in the beginning of this section. In Fig. 2(a), the solid curve represents the total absorption for a given J for these excited states. The dotted lines represent that of $L'=L-5$ (thick dots) and $L'=L+5$ (light dots) with $J=L=I\otimes L'$. The other L' values are as mentioned in the figures. As can be seen in the figures, the absorption for different L' values do not closely agree, especially for the $L-5$ and $L+5$ partial waves. This disagreement is less for the curves representing the $L-1$ and $L+1$ partial waves. Similar differences were shown for inelastic S-matrix in Fig. 1b of [5].

The results shown in Fig. 2(b) are obtained by switching off the imaginary part of the coupling potentials, whereas for Fig. 2(a) the full complex coupling potentials were used. The results using the isocentrifugal option in FRESCO calculations are shown in Fig. 2(b) labeled by ICA for $J=L-5$ and $L+5$ cases. The results using ICA show less absorption for $L-5$ curve and more for the $L+5$ case compared to exact calculations. The total absorption in Pb excited state, summing over all the subchannels of angular momentum are also shown for the exact calculation and the ICA method [see curves labeled total in Fig. 2(b)]. The ICA yields acceptable

results for the total absorption cross sections of Fig. 2(b), even though this approximation is not valid within this partition especially for low J values and higher spins at higher energies. The difference in absorption within a partition is due to the different centrifugal barriers in these channels. This difference (ICA) is enhanced for the second coupling scheme and also by the Coulomb couplings. The total contribution to fusion is insensitive to the relative differences shown in Fig. 2(b). The total absorption of Fig. 2(b) is not proportional to the absorption from any of the subchannels presented in the figure. However, the total may be given by an effective one channel with $L'=J=L$. Fusion of column 6 of Table I is not much effected by the ICA also because its major contribution arises from the coupled elastic channel. Therefore this approximation is consistent with the full CC calculations for fusion as shown in [3,4,6]. It should be noted that this approximation is very valuable for the fusion models.

The ratios of absorption from each channel of the coupling scheme to the total absorption have been studied as a function of energy. The ratio $\sigma_{a,\mathrm{el}}/\sigma_{a,D}$ falls with increasing energy, showing the increasing importance of absorption from other channels. The diagonal absorption from excited states of Pb increases at higher energies.

The absorption matrix (AM) of flux from the coupled channels system has been presented from deep sub-barrier energies to high energies. The absorption matrix method is found to be well suited for fusion at low energies, where the difference of cross sections (PS) method presently used in some CC codes is unreliable. The AM method is used to derive the contributions to fusion spin distribution from each physical channel included in the coupling scheme. The decomposition of the total fusion spin distribution into its various constituents has been presented for a comparison. It is shown that the maximum absorption takes place from the coupled elastic channel. For the case of complex coupling potentials, the absorption from the transition terms is significant and comparable to the diagonal absorption. The total absorption for the cases of purely real and the complex coupling potentials did not show any difference. Therefore, deformation of the short ranged imaginary potentials in CRC calculations may be ignored without effecting the CRC results. The flux absorbed in the various angular momentum subchannels of a given total J differ significantly, implying that the isocentrifugal approximation is not generally valid within a partition for higher spins. However, this approximation did not effect the total fusion and this aspect has been discussed.

I am thankful to Dr. S. S. Kapoor, Dr. S. Kailas, Dr. R. K. Choudhury, Dr. A. K. Mohanty, and Dr. A. Navin for their support during this work.

[1] C. H. Dasso and S. Landowne, Comput. Phys. Commun. **46**, 187 (1987).
[2] K. Hagino, N. Rowley, and A. T. Kruppa, computer code CCFULL, Comput. Phys. Commun. **123**, 143 (1999).
[3] R. J. Cross, J. Chem. Phys. **85**, 3268 (1986).
[4] O. Tanimura, Phys. Rev. C **35**, 1600 (1987).
[5] M. A. Nagarajan, N. Rowley, and R. Lindsay, J. Phys. G **12**, 529 (1986).
[6] R. Lindsay and N. Rowley, J. Phys. G **10**, 805 (1984).
[7] M. Dasgupta, D. J. Hinde, N. Rowley, and A. M. Stefanini, Annu. Rev. Nucl. Part. Sci. **49**, 401 (1998).
[8] J. Raynal, Phys. Rev. C **23**, 2571 (1981); *Computing as a Language of Physics* (IAEA, Vienna, 1972), p. 281.
[9] I. J. Thompson, Comput. Phys. Rep. **167**, 7 (1988).
[10] S. V. S. Sastry, S. K. Kataria, A. K. Mohanty, and I. J. Thompson, Phys. Rev. C **54**, 3286 (1996).
[11] G. R. Satchler, M. A. Nagarajan, J. S. Lilley, and I. J. Thompson, Ann. Phys. (N.Y.) **178**, 110 (1987).
[12] G. R. Satchler, Phys. Rep. **199**, 147 (1991).
[13] G. R. Satchler, *Direct Nuclear Reactions* (Oxford University, New York, 1983), pp. 617, 647.